High-Speed Railway Communication System Using Linear-Cell-Based Radio-Over-Fiber Network and Its Field Trial in 90-GHz Bands

Atsushi Kanno, *Member, IEEE*, Pham Tien Dat, *Member, IEEE*, Naokatsu Yamamoto, Tetsuya Kawanishi, *Fellow, IEEE*, Nagateru Iwasawa, Nariya Iwaki, Kazuki Nakamura, *Member, IEEE*, Kunihiro Kawasaki, *Member, IEEE*, Naoki Kanada, Naruto Yonemoto, *Member, IEEE*, Yosuke Sato, Masato Fujii, Katsuya Yanatori, Nobuhiko Shibagaki, and Kenichi Kashima

(Post-Deadline Paper)

***Abstract*—A linear-cell-based radio-over-fiber (LC-RoF) system is proposed and demonstrated for efficient mobile communication in high-speed trains without hard handover processes. The configuration of the LC-RoF network and possible router architectures are discussed for the field trial test of the proposed system and for advanced systems in the future. Via the LC-RoF network, 90-GHz, millimeter-wave radio access between the ground and a train car is operated in a centralized manner. The resulting throughput of 1.5 Gbit/s is achieved in the field trial test, which is comprised of 250-Mbaud four-subcarrier differential quadrature phase-shift keying with a forward-error correction code implemented in field-programmable gate arrays to the Shinkansen train traveling at 240 km/h without any interruptions in the connections at the change of radio access units.**

***Index Terms*—Millimeter-wave radio communication, radio over fiber, rail transportation communication.**

Manuscript received June 1, 2019; revised July 24, 2019; accepted September 23, 2019. Date of publication October 10, 2019; date of current version December 30, 2019. This work was supported in part by the project entitled "Research and development of millimeter-wave backhaul technology for high-speed vehicles," funded by the Ministry of Internal Affairs and Communications, Japan. *(Corresponding author: Atsushi Kanno.)*

A. Kanno, P. T. Dat, and N. Yamamoto are with the Network System Research Institute, National Institute of Information and Communications Technology, Tokyo 184–8795, Japan (e-mail: kanno@nict.go.jp; ptdat@nict.go.jp; naokatsu@nict.go.jp).

T. Kawanishi is with the Network System Research Institute, National Institute of Information and Communications Technology, Tokyo 184–8795, Japan, and also with the Waseda University, Tokyo 169–8555, Japan (e-mail: kawanishi@waseda.jp).

N. Iwasawa, N. Iwaki, K. Nakamura, and K. Kawasaki are with the Railway Technical Research Institute, Tokyo 185–8540, Japan (e-mail: iwasawa.nagateru.81@rtri.or.jp; iwaki.nariya.73@rtri.or.jp; nakamura.kazuki.26@rtri.or.jp; kawasaki.kunihiro.29@rtri.or.jp).

N. Kanada and N. Yonemoto are with the Electronic Navigation Research Institute, National Institute of Maritime, Port, and Aviation Technology, Tokyo 181–0004, Japan (e-mail: kanada@mpat.go.jp; yonemoto@mpat.go.jp).

Y. Sato, M. Fujii, K. Yanatori, N. Shibagaki, and K. Kashima are with the Hitachi Kokusai Electric Inc., Tokyo 187–8511, Japan (e-mail: sato.yosuke@h-kokusai.com; fujii.masato@h-kokusai.com; yanatori.katsuya@h-kokusai.com; shibagaki.nobuhiko@h-kokusai.com; kashima.kenichi@h-kokusai.com).

Color versions of one or more of the figures in this article are available online at http://ieeexplore.ieee.org.

Digital Object Identifier 10.1109/JLT.2019.2946691

I. Introduction

UBIQUITOUS connectivity to the Internet from anywhere and anytime is now indispensable for using smart devices based on mobile communication services, such as the fourth-generation (4G) mobile-communication system. 4G mobile communication services have been started in more than 80 countries, and now, the fifth-generation (5G) mobile service has also been launched [1]–[3]. In the emerging 5G era, high throughput and low-latency features will enhance the connectivity of many Internet-based activities such as playing network-based side-by-side games, watching 4K movies, among others. Such "kill-time" activities are highly demanded during a long journey by airplanes and during long-haul rails [4]. Particularly, in high-speed-train journeys for long distance, high Internet connectivity is a key factor because nowadays almost all the passengers can use their smart devices to access Internet services. However, the current railway communication systems (RCSs) used as a passenger service are provided via 4G mobile communication systems, satellite communications, and broadband wireless access systems such as the WiMAX [5]. In mobile communication-based systems, including the WiMAX, the size of a coverage cell could be up to 1–2 km to provide sufficient throughput greater than 20 Mbit/s. However, in this case, high-speed trains such as the Japanese Shinkansen with speed up to 300 km/h, or even a Maglev-system-based train with speed up to 500 km/h, pass the coverage cell in just 10 sec. Consequently, the hard handover (handoff) process, which performs the change of base transceiver stations that connect terminal devices, often occurs, and finally, thereby dramatically degrading the effective throughput: typical hard handover time would be achieved at least every several hundred of milliseconds and last up to several seconds [6]. For the reduction of the handover time, a linear-cell system has been proposed and discussed to remove the hard handover process in RCSs [7]–[10]. In fact, a train car runs on a railway track, which is configured linearly; on the contrary, a typical mobile-communication system requires cell coverage in a two-dimensional manner. Moreover, linear-cell systems enable to install a radio access unit (RAU) just along the railway track; thus, a

back-end network based on the optical-fiber communication can be easily deployed using both star-type and bus-type topologies.

For an increase in the throughput, an increase in the carrier frequency in the wireless domain (ground-to-train (G2T) and train-to-ground (T2G)) is indispensable for the realizing a broad bandwidth. A millimeter-wave radio at a frequency greater than 60 GHz is a possible radio band to provide 1 Gbit/s or more as a throughput. For application to a wireless local access network system, the IEEE802.11ad has been established with a throughput up to 7.2 Gbit/s in the 60-GHz band [11]. However, atmospheric attenuation and high free-space path loss, which are inversely proportional to the square of the signal wavelength, induce high transmission loss in millimeter-wave radio systems, thereby dramatically shortening the coverage cells length; furthermore, frequently occurring hard handover may force to fail the establishment of the connection [12]. In addition, the small size of a coverage cell size requires installing a large number of RAUs. In this scenario, the transceiver with a baseband processor (BB Proc.), which performs modulation, demodulation, and transmission-impairment compensation of the signals via digital-signal-processing scheme, cannot be implemented in each RAU because of its cost and footprint. In 4G- and 5G-based mobile communication, a centralized radio access network (C-RAN) is discussed and being implemented in the microwave frequency bands [13]. Under such a bandwidth-limited condition, a digitized optical-fiber-communication system is feasible for the transceivers optimal functioning. However, a millimeter-wave radio with a throughput greater than 1 Gbit/s induces insufficient capacity in the digitized transmission system, such as a common public radio interface [14]. The radio-over-fiber (RoF) technology, particularly the analog RoF technology, is a promising solution to deliver radio signals to remote sites under the C-RAN configuration [15], [16]. A millimeter-wave RoF system was discussed and demonstrated with capacity greater than 50 Gbit/s [17]–[19]. Many components in optical-fiber-communication systems can be adapted with moderate costs, which makes the RoF-based C-RAN system a feasible solution for realizing high-capacity RCS in the millimeter-wave bands [20]–[23].

In this study, we configure a linear-cell-based RoF network that empowers the millimeter-wave radio access system. Furthermore, automatic train tracking based on the network switch in the RoF network is implemented and demonstrated in the field trial test [24], [25]. 90-GHz millimeter-wave radio access communication between the ground and train is established under the RoF network by using centralized path control. In this paper, we introduce the concept and its expected system diagram in Sec. II. A possible solution of network-switch techniques and the RoF signal formation are discussed for the field trial system and future-based advanced systems. In Sec. III, the systems setup and obtained results from the field trial on the Hokuriku Shinkansen railway route are shown and discussed for demonstrating the systems feasibility.

II. Concept and System Diagram

A linear-cell-based system is configured using radio coverage cells connected linearly on the railway tracks, not two-dimensionally. Highways and airport runways are also covered by the linear-cell-based system. In these systems, we can predict the terminals location and movement easily because the movement of the terminal is generally one-way. On the other hand, in typical mobile-communication systems, the terminal held by the personnel could be randomly moved two-dimensionally. Therefore, prospective preparation for the change of the cell cannot be performed. Railway systems, particularly high-speed-rail systems, have an operation direction center to control the traffic of the trains, which gathers train-location information (TLI), the velocity of the train cars, congestions of the train operation, among others via an operation radio system [26]. In the scenario, the successive location of a train can be easily predicted based on the TLI. Thus, the agile control of the path routes in RAU-connected networks realizes the tracking of the train car. In other words, a "virtual" base station is traveled along with the train car by an adaptive change of the path route. Finally, the centralized control of the RAUs installed in the linear-cell-based system by using the TLI received in the direction center realizes uninterrupted connections between the ground side and the train car.

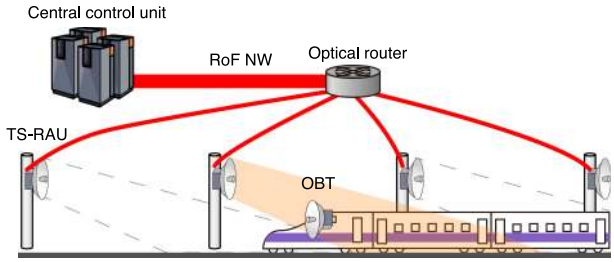

Fig. 1. Conceptual schematic of LC-RoF system for high-speed railway communication system.

Fig. 1 depicts a schematic of a linear-cell-based RoF (LC-RoF) network for the high-speed railway communication system. A central control unit (CCU) is equipped with optical transceivers to deliver radio signals into track-side RAUs (TS-RAUs). The RoF network based on an optical-fiber network is utilized as a point-to-multipoint radio signal feeder. Typically, a point-to-point link between the CCU and each TS-RAU can easily secure the feeder link; however, there is a lack of scalability in an increase of a number of the TS-RAUs. In addition, radio interferences could increase upon the activation of all the TS-RAUs. Therefore, the agile activation of the TS-RAU by feeding the signal from the CCU to the TS-RAU near the train car is realized by establishing a logical point-to-point link. Active optical-path routing by an optical router can deliver the signal to the TS-RAUs that are desired to be activated. When the train car passes the activated radio coverage cell, the adjacent coverage cell is also activated by the change of the path route for the signal transport. In this configuration, the TS-RAUs not connected to the control unit stop the irradiation of the radio signals, which result in effective reduction of the radio interferences and moreover, in the reduction of the total energy consumption of the system.

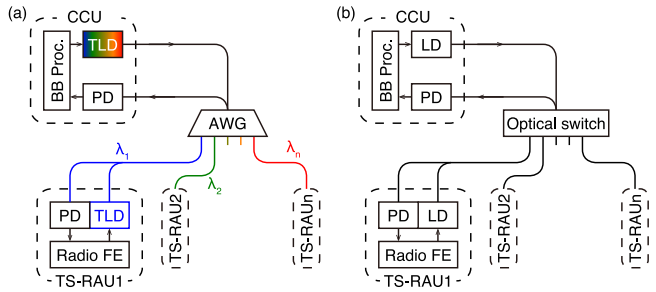

Fig. 2. Network configuration using (a) WDM-based optical router and (b) optical-switch-based router.

A. Network Configuration

To configure the LC-RoF network, particularly to realize the discussed train-tracking feature, we should take into account the configuration of the optical routers function. We have two simple solutions: the wavelength-division-multiplexed (WDM) routing and the optical-switch-based routing (see Fig. 2). The detail and examples of the solutions are described as follows.

1) WDM-Based Routing: The WDM system is widely used in terrestrial optical-fiber communication systems because of its possibly high capacity features, and the moderate costs of the required devices and components. Fig. 2(a) depicts an example of the WDM-based network configuration for the LC-RoF system. The CCU is comprised of a BB Proc., a wavelength-tunable laser diode (TLD), and a photodiode (PD). The TS-RAU has a similar configuration to that of a radio frontend instead of that of the BB Proc. Each TS-RAU is assigned with a wavelength channel (λ_n) for performing the WDM routing. In the scenario, to change the path in the network, the wavelength of the signal is adaptively changed in the network. In a downlink from the CCU to the TS-RAU1, for instance, the TLD in the CCU set at a wavelength λ_1 generates the signal into the network. The WDM router configured with an arrayed waveguide grating (AWG) distributes the signal to the assigned TS-RAU. For the uplink from TS-RAU1 to the CCU, the preset TLD at an operating wavelength of λ_1 provides the signal at a wavelength matched in the AWG. Finally, a bidirectional link can be established. The capacity of the TS-RAUs is a key factor for reducing the number of optical fibers and maintaining the connections between the CCU and the train car. A typical WDM configuration with the WDM grid of 50 GHz can receive 80 or more TS-RAUs in the optical C bands, by opting for more than 160 channels in the 25-GHz WDM grid [27]. In addition, the static WDM router can enhance the robustness and reduce system-configuration cost; however, the instability of the wavelength of the TLD may induce the failure of the link connection. However, the downlink from the CCU to the TS-RAU does not matter because the CCU is already set in a building near the train station, and thus, the ambient temperature around the TLD could be stabilized.

On the other hand, the TS-RAU is typically installed outdoor; the thermal instability of the TLD results in fluctuation in the wavelength of the uplink signal from the TS-RAU to the CCU. Particularly, in the dense WDM configuration, the wavelength fluctuation directly affects the probability of the establishment of the link. To solve the link-establishment issues, all the TLDs should be equipped with a wavelength tracker and stabilization function of the wavelengths.

The wavelength-fluctuation rate of the TLD in the CCU limits the switching speed of the TS-RAUs. Typical TLDs have a settling time of the wavelength of tens of milliseconds. On the other hand, a modulated-grating Y-branch laser diode (LD) is a possible solution for a quick wavelength fluctuation in the WDM system [28], [29]. This LD has a two-sectioned gain medium with a Y-branch coupler. When control currents are injected into a modulated-grating section to change the selection of the wavelength, a wavelength component is oscillated to irradiate from an output coupler of the device. Because the response time of the grating injected by the control currents is as quick as 10 s of microseconds, an ultrafast wavelength-tunable laser system can be developed. The obtained settling time is achieved to be smaller than 10 μs. Therefore, uninterrupted communication with a packet guard time of hundreds of microseconds can be performed.

Besides, the WDM configuration enhances the functionality of the network. For example, the development of the diversity system by using multi-onboard terminals (OBTs) is a promising way to retain the connectivity between the TS-RAU and the train car, particularly at the edge of the coverage cell. The OBTs can be set on the head and tail of the train car. In the case, two TS-RAUs are simultaneously activated to deliver the signals. The insertion of additional transceiver including TLD, PD, and BB Proc. helps realize the diversity configuration without any changes in the router. In the scenario, the WDM configuration is favorable to be implemented for use in advanced railway communication networks.

2) Optical-Switch-Based Routing: The optical-switch-based routing is a traditional way to change the optical path in a communication network. A time-division-multiplex-based routing technique seems suitable for implementing the train-tracking network. Fig. 2(b) depicts a schematic of the configuration. As compared with the WDM system, simple LDs without any wavelength-tuning fluctuation can be implemented in the CCU and in the TS-RAUs. On the other hand, the optical router is comprised of optical switches, which are an active component of the optical router, to change the path. The switching speed of the network is limited by the speed of the optical switch, which takes typically 10 s of milliseconds or less to perform switching. However, high capacity of the TS-RAUs requires multiple output ports of the switches; for example, 80 TS-RAUs can be received by performing 1×80 switches. The footprint of the switch may not hit the requirements of the installation. In addition, the link-diversity configuration mentioned above requires the installation of the switch fabric additionally. Therefore, from the scalability viewpoint, the WDM-based system is more favorable than the optical-switch-based one. However, the logical point-to-point link topology with physically point-to-multipoint networks can be easily designed using the optical-switch-based system. Moreover, simple and low-cost LDs can be implemented for many TS-RAUs. Therefore, the optical-switch-based system is more suitable for a proof-of-concept system and for relatively low-speed train systems, because a small number of the TS-RAU reception induces hard handover processes by changing the CCUs. Furthermore, infrequent processes in passing the train

car may lose the requirements of the system, with moderate costs of the switch fabrics. In this study, for performing the field trial test, we use the optical-switch-based routing system for four TS-RAUs.

B. RoF Signal Formation

In the LC-RoF network, the formation technique of the RoF signal is also a key factor for the implementation of the system in the field and future advanced systems. In this section, we explain a typical intermediate frequency (IF) over fiber system for the millimeter-wave radio communications and the frequency-multiplication-applicable signal formation technique for THE expected cost reduction in the future advanced system.

1) IF-Over-Fiber Configuration: The RoF technique to form the radio signal is just based on optical heterodyne technique, which generates radio signals at a frequency corresponding to the frequency difference between two optical signals. To generate the millimeter-wave signal, for example, two optical signals comprised of the baseband optical component and optical reference component should have a frequency separation in the millimeter-wave bands. In this case, spectral efficiency in the optical domain is limited because of its frequency separation, as a 100-GHz bandwidth is required in generating a 100-GHz RoF signal. As mentioned above, for achieving high capacity in the WDM system, the optimization of the spectral efficiency is indispensable to receive a large number of the TS-RAUs. An IF-over-fiber configuration can enhance the spectral efficiency. An RoF signal at an operating frequency in the IF domain would have the frequency separation with the IF frequency, following which the frequency conversion using an electrical heterodyne system at the TS-RAU up-converts the IF signal into the millimeter-wave signal. Additional fabric, such as a millimeter-wave mixer and a local oscillator (LO) synthesizer, in the TS-RAUs is required for performing the heterodyning; however, the development of 5G mobile-communication systems and advanced millimeter-wave communication and radar systems dramatically reduce the cost of the components. Therefore, at this time, the heterodyne-based IF-over-fiber system becomes feasible for implementation.

The selection of the suitable IF frequency is important for realizing the IF-over-fiber system. In the optical domain, particularly in optical-communication systems, fractional bandwidth need not be considered because the optical carrier frequency of 200 THz in the optical C-band is much higher than the baseband modulation frequency, even in the 100-GHz band. On the other hand, in the radio domain, the optimization of the fractional bandwidth in the system affects the availability of the radio components such as amplifiers and mixers. Typically, the fractional bandwidth of 10% or less is utilized to keep the flatness of the frequency response both in amplitude and phase components. Therefore, when the bandwidth of the millimeter-wave signal is assumed to be 1.5 GHz, a carrier frequency of the IF-over-fiber signal should be approximately 15 GHz. In the scenario, an optical-fiber chromatic dispersion results in degradation of the resultant RF throughputs under a double-sideband (DSB) modulation scheme: the throughput $\propto \cos(\pi L D \lambda^2 f^2/\nu)$, where L, D, λ, f, and ν denote optical-fiber length, dispersion coefficient

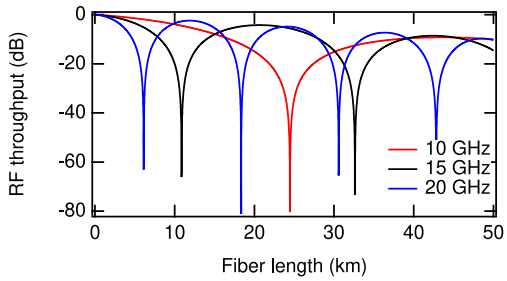

Fig. 3. Resultant RF throughputs, including fiber transmission loss of 0.2 dB/km, under DSB modulations at the RF frequency of (red) 10 GHz, (black) 15 GHz, and (blue) 20 GHz.

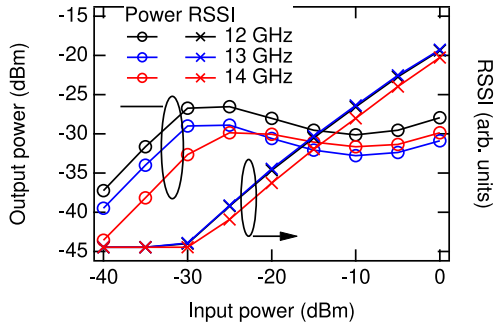

Fig. 4. Developed AGC-VGA characteristics at a frequency around 13 GHz. Resultant RSSIs in the field trial test are also shown.

of the fiber, wavelength of the optical signal, RF frequency, and the speed of light in the optical fiber, respectively [30]. In a typical single-mode fiber with D of 17 ps/nm/km at the frequency of 15 GHz, the RF throughput vanishes at an optical-fiber length of approximately 10 km (see Fig. 3). To deliver the signal in the high microwave band, a dispersion-tolerant scheme of modulation—single-sideband (SSB) modulation scheme—could be implemented. The SSB modulation scheme that uses an optical in-phase (I) and quadrature-phase (Q) modulator has been developed and demonstrated. An alternative technique that uses a combination of optical-intensity and phase modulators has been proposed and demonstrated in the IF-over-fiber system. Thus, the IF-over-fiber scheme is feasible for the radio-signal delivery in the RoF network.

For the downlink system from the CCU to the TS-RAU, the link gain and quality of the received signal can be easily optimized because the transmitted signal is prepared by the CCU. On the other hand, in the uplink system from the TS-RAU to the CCU, a received millimeter-wave signal is too weak, approximately $-$ 60 dBm, to drive the optical modulator for the signal generation in an IF-over-fiber system. Moreover, in the millimeter-wave section, a high dynamic range of the transmission loss, which is inversely proportional to the square of the wavelength of the radio signal, varies the reception signal strength with a dynamic range up to 30 dB or more. In the case, a variable-gain amplifier with an automatic gain controller (AGC-VGA) should be implemented for the uplink-signal modulation. Fig. 4 depicts a developed AGC-VGA characteristic in the input IF power range of $-$40–0 dBm. The AGC-VGA is configured using a 4-stage variable-gain attenuator and an

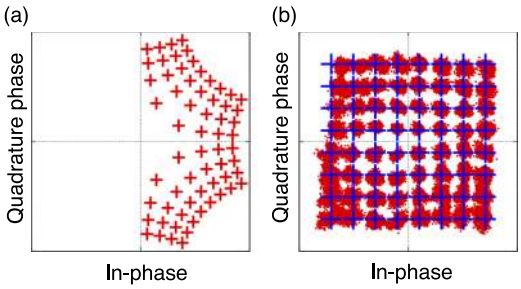

Fig. 5. (a) Designed constellation maps for 64-ary QAM under frequency-doubling system and (b) the obtained 64-ary QAM signal after performing the frequency doubling experimentally.

amplifier chain with a diode detector. Once the diode detector senses the input IF power level, the microcomputer-based AGC circuit optimizes the attenuator values in the VGA. In the input level of −30–0 dBm, the output-power level is stabilized with a power fluctuation of less than 6 dB. A received signal strength indicator (RSSI), which is kept linearly in the input range of −30–0 dBm, is employed in the TS-RAU equipment for the field trial described later. Finally, the 30-dB dynamic range is realized in the input of the IF modulator for the uplink system. Both downlink and uplink systems could be configured using the IF-over-fiber system.

2) Optical Frequency Multiplication Based Formation: The IF-over-fiber system is a reasonable solution for transportation of communicating sicnal to remote sites; additional components in the TS-RAU may increase complexity in the system. A frequency-multiplication technique is developed and used for the millimeter-wave radar system based on DSB suppressed-carrier (DSB-SC) modulation. A carrier-less heterodyne detection in the RoF link multiplies the resultant frequency at the reception by a PD [31], [32]. In the scenario, a moderate IF signal input into the optical-intensity modulator directly provides the millimeter-wave signal with low complexity in the TS-RAU. In addition, the fiber chromatic dispersion effect is negligible because of the existence of just two optical components in the optical domain [33]. The radar transceiver is typically configured using the multiplication-based frequency upconversion scheme, and thus, the diversion of the millimeter-wave transmitter from the well-developed radar system can be realized to achieve cost reduction.

For the generation of the signal for the frequency-multiplication-based RoF system, the symbol assignments in the multilevel constellation map should be realigned. Particularly, in the DSB-SC modulation scheme, which provides frequency doubling, the symbol constellation for the transmitter is relocated by second-root form from the expected maps, as depicted in Fig. 5. Remapping the constellation can be calculated in online using a field-programmable gate array (FPGA). The obtained 64-ary quadrature amplitude modulation (QAM) signal after performing the frequency doubling in the millimeter-wave bands with an estimated error vector magnitude of approximately 7%. The observed distortions in amplitude and phase could be caused by the millimeter-wave amplifier set after the PD. This concept is generalized and applicable not only to single-carrier multilevel modulation but also to a multi-carrier system such as an orthogonal frequency-division multiplexing system. Moreover, higher-order multiplication, such as a multiplication factor of 4 or more, could be feasible if the dynamic range and resolution of a vector signal generator are high enough, which means possibly high spectral efficiency with low-cost and well-developed transceivers, which are suitable for implementation in future millimeter-wave and terahertz-wave communication systems.

III. Field-Trial Demonstration

To evaluate the concept of the LC-RoF system, we tried the field trial test in Shinkansen, which is a high-speed railway network in Japan. The trial system was installed in the Hokuriku Shinkansen with the efforts of the West Japan Railway Company. First, we show the system diagram installed during the field trial, and then, the obtained results will be shown.

A. System Block Diagram

Fig. 6 depicts a system block diagram of the LC-RoF system in the field trial test [24]. The system consists of three parts: a CCU, TS-RAUs, and an OBT. It should be noted that the optical-switch-based router is implemented in the field trial system because of its robustness and availability to optical components. In addition, the maximum optical fiber length would be up to 4 km, and therefore, the direct-detection-based IF-over-fiber system is configured using a simple DSB modulation scheme, not the SSB scheme. The induction of the RF throughput degradation due to fiber chromatic dispersion effect is negligible for such short lengths of optical fiber.

In the CCU, a BB Proc. based on four FPGAs is used for generating 250-Mbaud single-carrier differential quadrature phase-shift keying (SC-DQPSK) signals, whose roll-off factor is 0.25. Two digital-to-analog converters connected to each FPGA provide I and Q baseband components. IQ mixers with LO synthesizers in clock sources form first-stage IF signals at the frequency components of 1.8, 2.2, 2.6, and 3.0 GHz for four SC-DQPSK signals, where the guard bandwidth between each frequency component is 400 MHz. The IF signals are combined using a coupler, following which a mixer connected to the clock sources upconverts the IF signal into second-stage IF components at a center frequency of 12.4 GHz with a total bandwidth of 1.45 GHz. The IF amplifier that is set after the mixer optimizes the input signal level into an optical Mach–Zehnder-interferometer-type intensity modulator (MZM). The MZM is operated using an LD at a wavelength of approximately 1550 nm. For the preparation of the IF-over-fiber signal for the transmission of data, the bias voltage of the MZM is set to a quadrature transmission point in the transfer function of the MZM by using the DSB modulation scheme. In the CCU of the trial system, the signals generated by the LO and millimeter-wave mixer in the TS-RAU are transmitted using a centralization manner. In the system, it is not necessary to install independent LO sources in the TS-RAUs. This scheme has the advantage of not only of the reduction of cost and footprint of the TS-RAUs but also the stabilization of the millimeter-wave frequency for

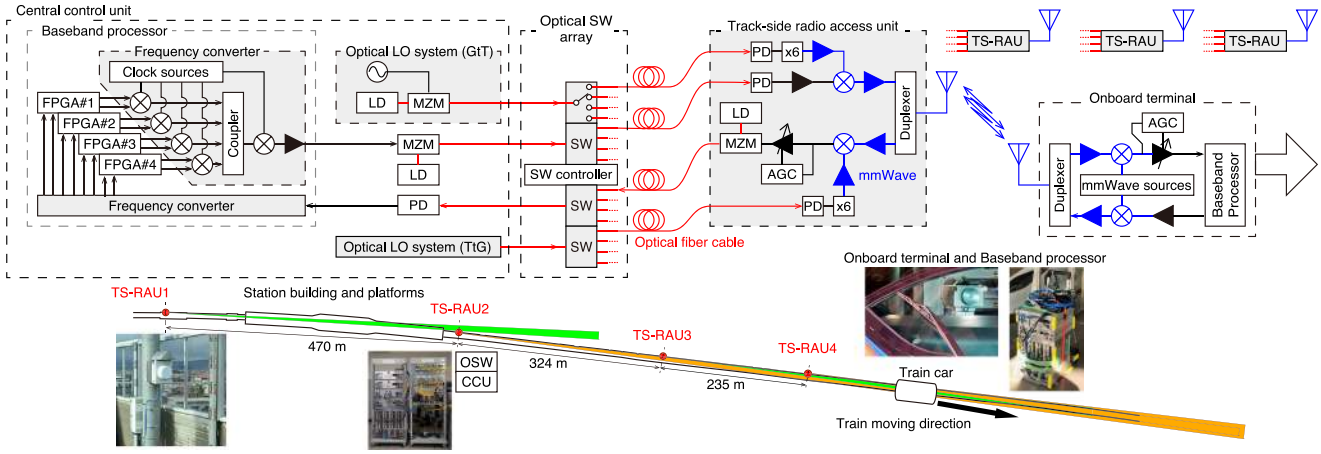

Fig. 6. Block diagram of the field trial system and the corresponding map of the trial field.

a (G2T) link. Moreover, the IF signals regenerated in the TS-RAU are also stabilized in the frequency domain. Therefore, the number of resources required in the FPGAs for performing carrier-frequency-offset compensation in the BB Proc. could be effectively reduced. In this field trial test, we used an optical LO signal transmitted from the CCU for the operation of the millimeter-wave mixer in the TS-RAUs. A shared LO configuration helps reduce the number of computational resources in the FPGA for performing frequency-offset compensation. The optical LO transmitter is comprised of the LD, MZM, and a synthesizer. DSB-based RoF signals are formed at an operating frequency of 13.8834 GHz for the G2T link and 14.35 GHz for the (T2G) link. Two optical LO sources and the IF-over-fiber signal are input into a switch fabric, i.e., an optical switch array (OSW). In the field trial system, four TS-RAUs are installed in the field, and therefore, four 1×4 switches are developed as the fabric: three for downlink (the CCU to the TS-RAU) and one for uplink (the TS-RAU to the CCU). After using the optical switches, three optical-fiber cables are used for the downlink, to connect to the TS-RAU.

In the TS-RAU, we configured the heterodyne (coherent) based transceiver in the millimeter-wave domain, as a direct-detection-based system was configured in the optical domain. The PD for the IF-over-fiber signal converts the signal into the 12.4-GHz-centered IF signal. After optimizing the signal level, a millimeter-wave upconversion mixer converts the signals frequency from 12.4 to 95.7 GHz. In the LO of the mixer, the frequency of the 13.8834-GHz LO signal, which was converted by the PD from the optical LO system, was multiplied with the multiplication factor of 6. As a result, a 83.3004-GHz millimeter-wave LO signal is launched into the mixer. Afterward, using a millimeter-wave amplifier and a frequency duplexer, a 95.7-GHz millimeter-wave signal is irradiated via an antenna into the air. On the other hand, in the T2G link, the antenna collects the incoming millimeter-wave signal at a frequency of 98.5 GHz. After the frequency duplexing of the transmitted and received signals, a frequency-downconversion mixer converts the received signals frequency from 98.5 to 12.4 GHz using the optical LO signal at a frequency of 14.35 GHz; the signals frequency is finally converted to 86.1 GHz using the $\times 6$ multiplier. The power level of the downconverted IF signal is optimized using the AGC-VGA mentioned above to remain constant. Finally, the MZM connected to the LD generates the DSB IF-over-fiber signal at the frequency of 12.4 GHz. For the receiver in the CCU, the PD converts the IF-over-fiber signal passing through the OSW to the analog IF signal. Finally, the frequency converter in the baseband processor, which is comprised of the similar components for the transmitter, provides four IQ signals. The FPGAs perform online signal processing to demodulate and compensate the received signals.

In the OBT, the same components as those used in the CCU, without any optical fibers, are used for the baseband processors. The AGC-VGA is also used for optimizing the level of the received signal. The baseband processors both in the CCU and OBT are connected to a personal computer to gather the information of the throughput, the RSSI, and demodulated symbol constellation map, via an Ethernet connection. Keeping the connectivity via the Ethernet between the PCs in the CCU and in the OBT, the Ethernet frame is reformed into an IF packet frame, which is achieved by encapsulating the Ethernet packet into the IF signal packet. Furthermore, error correction is performed using a forward error correction FEC code based on a shortened Reed–Solomon code ($N = 255$, $K = 239$, and $S = 67$), processed in the FPGA. The estimated total overhead of the transmission signal is approximately 1.33.

The installation location of the four TS-RAUs are also indicated in Fig. 6. The separation between the TS-RAUs is set as 235–470 m because of the limitation of the construction. For a Cassegrain-antenna unit, the 3-dB beamwidth of the millimeter-wave signal from the TS-RAU is approximately 1 degree, which corresponds to the antenna gain of 42 dBi; however, for an OBT antenna, the 3-dB beamwidth of the millimeter-wave signal from the TS-RAU is 2 degrees, which corresponds to the antenna gain of 35 dBi. It should be noted that such a narrow beam causes a radio quiet zone by the platform structure in the station as well as on the curvature of the railway track. Actually, the TS-RAU1 in Fig. 6 has small coverage because of these structural issues. The CCU and the OSW are set in a building near the train station.

In this field trial test, the TLI could not be provided from the direction center to control the states of the OSW. Therefore, a laser sensor to detect passing the train car is equipped in each TS-RAU. After the train car passing the TS-RAU, the laser sensor is activated to send the clock to an optical switch controller via a control network based on an optical 10-GbE-based system. The controller receiving the clock signal from the TS-RAU changes the state of the OSW; the optical path in the RoF network is changed to the path for the next TS-RAU. Since the OBT is set in a rear driver cabin of the train car, as compared with the TLI, this control scheme tracks the train car automatically.

In this trial, 90-GHz bands are discussed and implemented. Actually, a 94.1–100 GHz frequency band is assigned as a land-mobile service in the Radio Regulations, thereby providing bandwidth of 5.9 GHz [34]. On the contrary, the 60-GHz band has broader bandwidth of 7–9 GHz including license-free industry, science and medical, i.e., ISM, radio bands of 61–61.5 GHz; however, the atmospheric-attenuation coefficient is ten times as high as that in the 90-GHz bands. Therefore, for middle-range, high-throughput transmission, 90-GHz band is one of the promising bands at the frequency of less than 100 GHz.

Considering radio communication system for high-speed vehicles, a Doppler shift of the millimeter-wave carrier frequency may degrade the signal quality. Actually, the Doppler shift of 95.7-GHz millimeter-wave signal frequency induced by the 240-km/h train is estimated approximately as 21 kHz and can be easily mitigated by performing carrier-frequency-offset compensation by digital signal processing in the FPGA. It should be noted that the linewidth of the LDs does not directly affect millimeter-wave signal quality, as the phase noise of the clock sources and baseband signals in this system is small enough for 250-Mbaud DQPSK demodulation in the 90-GHz band.

B. Results

For evaluating the baseband and millimeter-wave signal quality, Fig. 7 depicts the electrical power spectra in the IF band and millimeter-wave bands. The obtained spectrum for the IF signal shows clear subcarrier separations with a 400-MHz spacing. On the other hand, in the 90-GHz bands, each subcarrier component measured independently is clearly separated; however, in the total spectra, no gap is observed between subcarriers 2 and 3 because of the harmonic spurious, a non-essential characteristic in the system, caused by the harmonic mixer used for spectrum measurement. Adjacent rolls near subcarriers 1 and 4 could be caused by an intermodulation distortion by four subcarriers induced by the millimeter-wave amplifier. The resultant signal-to-noise power ratio, which is greater than 25 dB, is high enough to demodulate the signals. As the frequency separation between the G2T (95.7 GHz) and T2G (98.5 GHz) signals is 1.5 GHz, the duplexer installed in the TS-RAU and the OBT can successfully split the signal in a frequency-division duplexing manner.

In the optical domain, the IF and optical LO signals are successfully generated, as depicted in Fig. 8. The RF signal for the IF-over-fiber signal and the LOs are operated at a frequency approximately 13 GHz, and thus, an optical spectrum analyzer

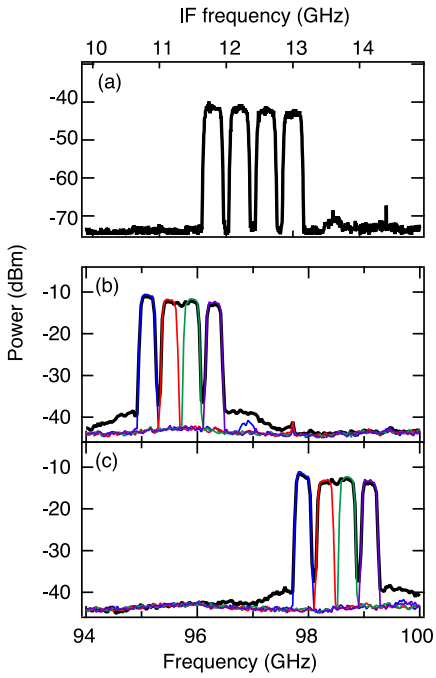

Fig. 7. Electrical power spectra of (a) the IF signal measured at the input to the MZM in the CCU, (b) the 95.7-GHz G2T signal, and (c) the 98.5-GHz T2G signal. In (b) and (c), the black solid lines and colored lines denote the results of the simultaneous measurement of the four subcarriers and independent measurement in each subcarrier, respectively.

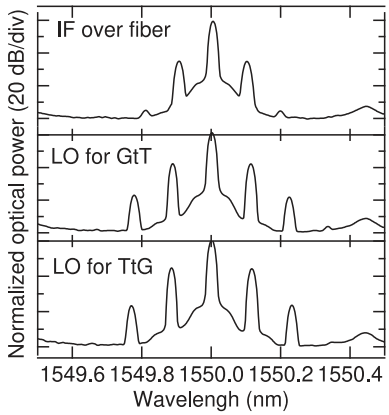

Fig. 8. The obtained optical spectra measured at the output from the CCU for (top) the IF-over-fiber signal, (middle) optical LO for the G2T link, and (bottom) optical LO for the T2G link.

could not identify the frequency component, owing to the resolution of approximately 10 GHz. For the IF-over-fiber signal, an optical modulation index (OMI) is smaller than that in the LO because the linearity of the IF-over-fiber signal should be kept high to transmit the SC-DQPSK signal. On the other hand, the OMIs for the optical LOs are set higher for an increase of a link gain in the optical fiber network. It should be noted that harmonic components are enhanced by a high OMI.

To evaluate the possible transmission range of the millimeter-wave signal from the LC-RoF-based TS-RAU, we tested the throughput and RSSI measurements under the activation of the TS-RAU2 only. Fig. 9 depicts the resultant data throughputs of

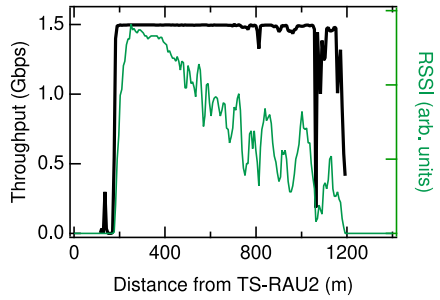

Fig. 9. Measured data throughput and the RSSI at a distance from TS-RAU2 under the activation of TS-RAU2 only.

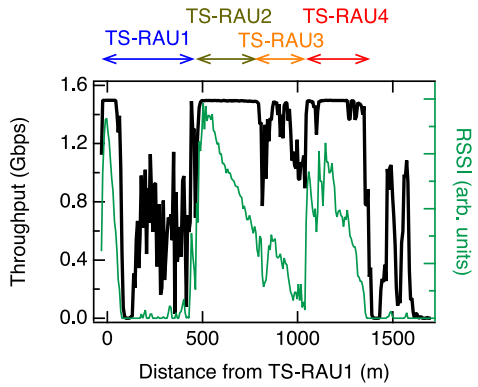

Fig. 10. The obtained throughput in the G2T link with the train car traveling at 240 km/h under four TS-RAU automatic tracking situations.

the G2T link. The obtained maximum throughput is achieved as 1.5 Gbps, which is evaluated at a net link rate of 2 Gbps (four 250-Mbaud DQPSK) with an overhead factor of 1.33. A successive link is established at a distance of 190–1200 m from TS-RAU2. The gradual degradation of the millimeter-wave signals RSSI also indicates the establishment of the link with a maximum transmission distance up to 1200 m from TS-RAU2. It should be noted that the throughput could not be obtained at a distance shorter than 190 m from TS-RAU2, because of the narrow beam of the millimeter-wave signal. The radio quiet zone can be compensated by the optimization of the location of the TS-RAUs; adjacent TS-RAUs can cover the coverage cell to mitigate the radio quiet zone.

The resultant throughput during 240-km/h Shinkansen train passing four TS-RAUs with an automatic path switching is depicted in Fig. 10, and the achieved maximum throughput is approximately 1.5 Gbps. There is no significant interruption of the throughput at the time of the change of the TS-RAUs. The RSSI degradation for TS-RAU3 is caused by the small misalignment of the TS-RAU antenna. It should be noted that the throughput has no significant degradation in the TS-RAU3 section, even if the RSSI is smaller than the aforementioned RSSI. This is because the throughput–RSSI dependence has a brick-wall-type behavior owing to the FEC; the throughput is dramatically degraded at the RSSI smaller than a threshold, although the throughput is constant when the RSSI is larger than the threshold. In the section covered by TS-RAU1, the throughput is strictly reduced because of the screening effect

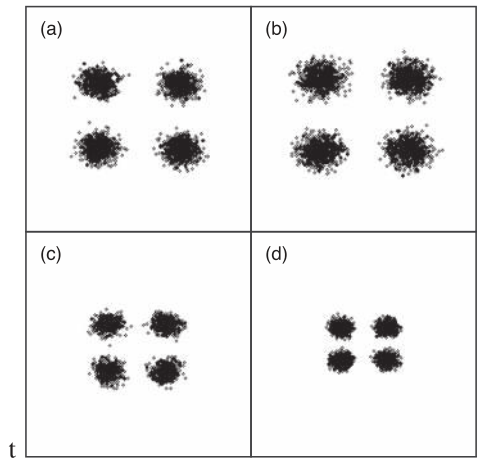

Fig. 11. The obtained constellation maps for (a) subcarrier 1, (b) subcarrier 2, (c) subcarrier 3, and (d) subcarrier 4 at a distance of 500 m from TS-RAU1 in Fig. 10.

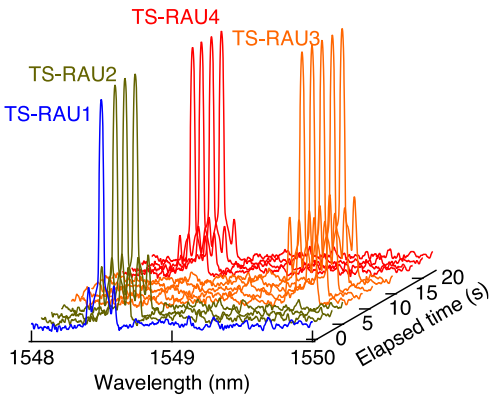

Fig. 12. Time-developed optical spectra during the Shinkansen train passing the TS-RAUs at 240-km/h. The line colors are indicated in Fig. 10.

from the platform structure (due to pillars and walls) and the curvature of the railway track, as depicted in Fig. 6. Fig. 11 depicts clear symbol separation in each subcarrier. In addition, the railway track with a curvature radius of 4000 m also causes the failure of the establishment of the link. In this field trial, the installation location of the TS-RAUs limits the design to keep the throughput. For the implementation in the commercial stage, this type of degradation will be mitigated by opting for the optimal design.

The behavior of the OSW is depicted in Fig. 12 as the time-varying optical spectra received at the CCU [35]. The OSW works well to change the TS-RAUs during the trains movement. As shown in the spectra by TS-RAU3, the sideband components remain constant for 7 sec. This is because of the AGC-VGA, which keeps the signal input level to the MZM constant. The obtained results show that the optical-switch-based routing works well for tracking the train car. In addition, the IF-over-fiber signal in each TS-RAU has various values of wavelength in the range 1548.5–1549.5 nm. The same LDs are used in all the TS-RAUs. However, environmental differences cause small changes in the wavelength, for example, a 0.1-nm change in the signal wavelength directly hits the WDM grid allocation; a

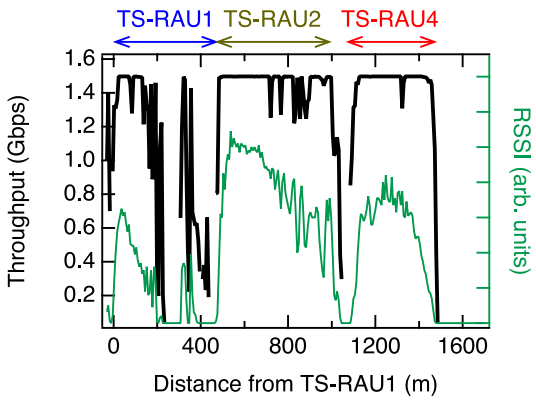

Fig. 13. The obtained throughput in the G2T link with the train car traveling at 240 km/h, under TS-RAU1, TS-RAU2, and TS-RAU4 activated.

200-GHz grid can be applicable for the 0.1-nm fluctuation. For the utilization of the WDM router scheme, the stabilization of the LD should be implemented.

Fig. 13 depicts an example of the throughput drop on the deactivation of TS-RAU3. The behaviors of TS-RAU1 and TS-RAU2 are similar to the situation depicted in Fig. 10. At the distance of 900 m from TS-RAU1, the throughput and the RSSI are sharply dropped, and finally, the link is broken. After the break, the Ethernet-based signal should be generated using a handshake procedure, thereby delaying the link establishment. These results show that an uninterrupted communication system is important to retain connectivity, as well as to decrease the delay induced by the handshake procedure.

IV. Conclusion

The LC-RoF system for high-speed and high-throughput RCS was proposed and demonstrated successfully. We discussed the following two types of LC-RoF networks for high-speed switching of the optical paths to track high-speed trains: wavelength-division multiplexing for high scalability and optical-switch systems for easy implementation. Also, we reviewed the RoF-signal-generation technique by using the IF-over-fiber system, and the multiplication-based systems for the simple implementation and possible cost reduction technique for future systems. In the field trial test, an IF-over-fiber transceiver connected to four TS-RAU that were installed along the railway track was implemented using an optical-switch-based router. The resultant throughput of 1.5 Gbit/s to the Shinkansen train car traveling at 240 km/h was achieved; the resultant throughput of 1.5 Gbit/s was observed to be consistent with that of four-channel 250-Mbaud DQPSK signals, which provide 2 Gbit/s in a line rate with the coding overhead of 1.33. As the throughput is limited by the speed of the FPGA and digital–analog interfaces, higher-order multilevel modulation with high symbol rate will provide higher throughput. As a result, an automatic network control to track the train car is successfully demonstrated using the LC-RoF system experimentally. This results using the LC-RoF-based C-RAN architecture in the 90-GHz bands will show advanced technique for the high-speed vehicle application proposed in the 5G mobile systems, although this frequency band is not considered in the 5G [36], [37]. The automatic network control technique in the RoF network with the millimeter-wave radio access system is highly expected to be a key technology for designing beyond 5G and 6G mobile communication systems.

Acknowledgment

We also thank the West Japan Railway Company for their great support in the field trial test.

References

[1] J. G. Andrews *et al.*, "What will 5G Be?" *IEEE J. Sel. Area Commun.*, vol. 32, no. 6, pp. 1065–1082, Jun. 2014.
[2] S. H. Won *et al.*, "Development of 5G CHAMPION testbeds for 5G services at the 2018 winter olympic games," in *Proc. IEEE Int. Workshop Sig. Proccess. Adv. Wireless Commun.*, Sapporo, Japan, Jul. 2017, Paper R2-1, pp. 1–5.
[3] National Instruments, "NI demonstrates worlds first real-time over-the-air prototype for verizon 5G at 28 GHz," Mar. 21, 2017. Online. Available: http://www.ni.com/newsroom/release/ni-demonstrates-worlds-first-real-time-over-the-air-prototype-for-verizon-5g-at-28-ghz/en/
[4] K.-D. Lin and J.-F Chang, "Communications and entertainment onboard a high-speed public transport system," *IEEE Wireless Commun.*, vol. 9, no. 1, pp. 84–89, Feb. 2002.
[5] S. Banerjee, M. Hempel, and H. Sharif, "A survey of wireless communication technologies & their performance for high speed railways," *J. Transp. Technol.*, vol. 6, pp. 15–29 2016.
[6] N. Nasser, A. Hasswa, and H. Hassanein, "Handoffs in fourth generation heterogeneous networks," *IEEE Commun. Mag.*, vol. 44, no. 10, pp. 96–103 Oct. 2006.
[7] B. Hamdaoui and P. Ramanatha, "A network-layer soft handoff approach for mobile wireless IP-based systems," *IEEE J. Sel. Area Commun.*, vol. 22, no. 4., pp. 630–642 May 2004.
[8] J. Wang, H. Zhu, and N. J. Gomez, "Distributed antenna systems for mobile communications in high speed trains," *IEEE J. Sel. Area Commun.*, vol. 30, no. 4, pp. 675–683 May 2012.
[9] A. Kanno, P. T. Dat, T. Kawanishi, N. Yonemoto, and N. Shibagaki, "90-GHz radio-on-radio-over-fiber system for linearly located distributed antenna systems," in *Proc. Photon. Global Conf.*, Singapore, Dec. 2012, pp. 1–5.
[10] H. Nishimoto *et al.*, "Linear cellularization enabling millimeter-wave train radio communication systems in 5G Era," in *Proc. Prog. Electromag. Res. Symp.*, Toyama, Japan, Aug. 2018, pp. 99–106.
[11] IEEE Std. 802.11ad-2012, "IEEE Standard for Information technology–Telecommunications and information exchange between systems–Local and metropolitan area networks–Specific requirements-Part 11: Wireless LAN Medium Access Control (MAC) and Physical Layer (PHY) Specifications Amendment 3: Enhancements for Very High Throughput in the 60 GHz Band," Dec. 2012.
[12] "Attenuation of atmospheric gases," International Telecommunications Union, Geneva, Switzerland, Recommendation ITU-R P.676-5, 2001.
[13] C.-L. I, J. Huang, R. Duan, C. Cui, J. Jiang, and L. Li, "Recent Progress on C-RAN centralization and cloudification," *IEEE Access*, vol. 2, pp. 1030–1039, 2014.
[14] Common Public Radio Interface (CPRI); Interface Specification, CPRI Specification V6.0, Aug. 30, 2013.
[15] C. Lim *et al.*, "Fiber-wireless networks and subsystem technologies," *J. Lightw. Technol.*, vol. 28, no. 4, pp. 390–405, 2010.
[16] K. Kitayama, "Coordinated role of optical and radio network in 5G-era," in *Proc. Int. Top. Meet. Microw. Photon.*, Paphos, Cyprus, Plenary talk, Oct. 2015, pp. 1–4.
[17] X. Pang *et al.*, "100 Gbit/s hybrid optical fiber-wireless link in the W-band (75–110 GHz)," *Opt. Express*, vol. 19, no. 25, pp. 24944–24949, 2011.
[18] A. Kanno *et al.*, "40 Gb/s W-band (75–110 GHz) 16-QAM radio-over-fiber signal generation and its wireless transmission," *Opt. Express*, vol. 19, no. 26, pp. B56–B63, 2011.
[19] X. Li, J. Yu, J. Zhang, Z. Dong, F. Li, and N. Chi, "A 400G optical wireless integration delivery system," *Opt. Express*, vol. 21, no. 16, pp. 18812–18819, 2013.
[20] Y.-T. Hsueh, M.-F. Huang, M. Jiang, Y. Shao, K. Kim, and G.-K. Chang, "A novel wireless over fiber access architecture employing moving chain cells and RoF technique for broadband wireless applications on the train environment," *Proc. Opt. Fiber Commun. Conf.*, Los Angeles, USA, Mar. 2011, Paper OWT3.

[21] H.-W. Chang, M.-C. Tseng, S.-Y. Chen, M.-H. Chen, and S.-K. Wen, "Field trial results for integrated WiMAX and radio-over-fiber systems on high speed rail," in *Proc. IEEE Int. Symp. Pers. Indoor Mobile Radio Commun.,* 2011, pp. 2111–2115.
[22] P. T. Dat, A. Kanno, N. Yamamoto, and T. Kawanishi, "WDM RoF-MMW and linearly located distributed antenna system for future high-speed railway communications," *IEEE Commun. Mag.*, vol. 53, no. 10, pp. 86–94 Oct. 2015.
[23] A. Kanno., P. T. Dat, N. Yamamoto, and T. Kawanishi, "Millimeter-wave radio-over-fiber network for linear cell systems," *J. Lightw. Technol.*, vol. 36, no. 2, pp. 533–540, 2018.
[24] A. Kanno *et al.*, "Field trial of 1.5-Gbps 97-GHz train communication system based on linear cell radio over fiber network for 240-km/h high-speed train," *Opt. Netw. Commun. Conf.*, San Diego, USA, Mar. 2019, Paper Th4C.2.
[25] K. Nakamura *et al.*, "The new ground to train radio communication system using 100 GHz band millimeter-wave," presented at the 12th World Congress of Railway Research, Nov. 2019.
[26] A. J. D. Santos, A. R. Soares, F. M. de Almeida Redondo, and N. B. Carvalho, "Tracking trains via radio frequency systems," *IEEE Trans. Intell. Transp. Sys.*, vol. 6, no. 2, pp. 244–258 Jun. 2005.
[27] P. T. Dat, A. Kanno, K. Inagaki, F. Rottenberg, N. Yamamoto, and T. Kawanishi, "High-speed and uninterrupted communication for high-speed trains by ultrafast WDM fiber-wireless backhaul system," *J. Lightw. Technol.*, vol. 37, no. 1, pp. 205–217, 2019.
[28] Y. K. Yeo, Z. Xu, C. Y. Liaw, D. Wang, Y. Wang, and T. H. Cheng, "A 448×448 optical cross-connect for high performance computers and multi-terabit/s routers," in *Proc. Opt. Fiber Commun. Conf.*, San Diego, USA, Mar. 2010, Paper OMP6.
[29] A. Kanno, P. T. Dat, N. Yamamoto, and T. Kawanishi, "Wavelength-switchable IF over fiber network under ultra-dense WDM configuration for high-speed railway systems," in *Proc. IEEE Photon. Conf.*, Orland, USA, Oct. 2017, pp. 591–592.
[30] K. J. Williams, "Microwave photonics: The past and the future," in *Proc. Opt. Fiber Commun. Conf.*, Anaheim, USA, Mar. 2013, Paper OTu2H.1.
[31] N. Kanada, N. Yonemoto, and T. Kawanishi, "92 GHz 64QAM signal generation by optical frequency doubler," in *Proc. IEEE Int. Top. Meet. Microw. Photon.*, Long Beach, USA, Oct. 2016, pp. 145–148.
[32] X. Li, J. Xiao, and J. Yu, "W-Band vector millimeter-wave signal generation based on phase modulator with photonic frequency quadrupling and precoding," *J. Lightw. Technol.*, vol. 35, no. 13, pp. 2548–2558, 2017.
[33] N. Kanada, N. Yonemoto, and T. Kawanishi, "Vector signal generation and transmission by radio over fiber system with frequency doubling at 96 GHz," in *Proc. SPIE 10559, Broadband Access Commun. Technol. XII*, San Francisco, USA, Jan. 2018, Paper 105590D.
[34] "Chapter II Frequencies," ITU Radio Regulations 2016 ed., Geneva: ITU, 2016.
[35] A. Kanno, P. T. Dat, N. Yamamoto, and T. Kwanishi, "Seamless converged network architecture based on fiber-wireless systems for high-speed train communication networks," Presented at the 12th World Congress of Railway Research, Nov. 2019.
[36] J. Rodriguez-Pineido, T. Domnguez-Bolano, P. Suarez-Casal, J. A. Garcia-Naya, and L. Castedo, "Affordable evaluation of 5G modulation schemes in high speed train scenarios," in *Proc. Int. ITG Worksp Smart Antenna*, Munich, Germany, pp, 476–483, Mar. 2016.
[37] L. Wang, T. Han, Q. Li, J. Yan, X. Liu, and D. Deng, "Cell-less communications in 5G vehicular networks based on vehicle-installed access points," *IEEE Wireless Mag.*, vol. 24, no. 6, pp. 64–71, Dec. 2017.

Atsushi Kanno (M'12) received the B.Sc., M.Sc., and Ph.D. degrees in science from the University of Tsukuba, Tsukuba, Japan, in 1999, 2001, and 2005, respectively. In 2005, he was with the Venture Business Laboratory of the Institute of Science and Engineering, University of Tsukuba. In 2006, he joined the National Institute of Information and Communications Technology, Tokyo, Japan. His research interests are microwave/millimeter-wave/terahertz photonics, ultrafast optical and radio communication systems, and ultrafast phenomena in semiconductor optical devices. He is a member of the Institute of Electronics, Information, and Communication Engineers, the Japan Society of Applied Physics, the Laser Society of Japan, the Institute of Electrical and Electronic Engineers, and the Society of Photo-Optical Instrumentation Engineers (SPIE).

Pham Tien Dat (M'12) received the B.Eng. degree in electronics and telecommunication engineering from the Posts and Telecommunications Institute of Technology, Ho Chi Minh City, Vietnam, in 2003, and the M.Sc. and Ph.D. degrees in science of global information and telecommunication studies from Waseda University, Tokyo, Japan, in 2008 and 2011, respectively. In 2011, he joined the National Institute of Information and Communications Technology, Tokyo, Japan. His research interests are in the field of microwave/millimeter-wave photonics, radio-over-fiber and optical wireless systems. He is a member of the IEEE Photonic Society.

Naokatsu Yamamoto received the Ph.D. degree in electrical engineering from Tokyo Denki University, Tokyo, Japan, in 2000. In April 2001, he joined the Communications Research Laboratory (now the National Institute of Information and Communications Technology, NICT), Tokyo, Japan. From July 2012 to September 2013, he was the Deputy Director with the Ministry of Internal Affairs and Communications. Since December 2013, he has been a Visiting Professor with Tokyo Denki University. He proposed many types of novel crystal growth techniques and successfully developed a QD optical frequency comb laser, an ultrabroadband wavelength-tunable QD laser, and heterogeneous QD photonic devices. He successfully demonstrated a high-speed and ultra-broadband photonic transport system constructed with novel nanostructured photonic devices. Recently, he has proposed the use of 1.0-μm waveband photonic transport systems to develop a novel optical frequency resource for optical communications. His research interests include nanostructured materials and IIIV semiconductor QD and their photonic device applications in photonic transport systems.

Tetsuya Kawanishi (M'06–SM'06–F'13) received the B.E., M.E., and Ph.D. degrees in electronics from Kyoto University, Kyoto, Japan, in 1992, 1994, and 1997, respectively. From 1994 to 1995, he was with the Production Engineering Laboratory of Panasonic. During 1997, he was with the Venture Business Laboratory, Kyoto University, Kyoto, Japan, where he was engaged in research on electromagnetic scattering and near-field optics. In 1998, he joined the Communications Research Laboratory, Ministry of Posts and Telecommunications (now the National Institute of Information and Communications Technology), Tokyo, Japan. During 2004, he was a Visiting Scholar with the Department of Electrical and Computer Engineering, University of California at San Diego, San Diego, CA, USA. Since April 2015, he has been a Professor with Waseda University, Tokyo, Japan. His current research interests include high-speed optical modulators and RF photonics. He is the TG-FWS (task group on fixed wireless systems) in AWG (Asia Pacific telecommunity wireless group).

Nagateru Iwasawa received the M.Eng. degree in information technology from the Tokyo University of Agriculture and Technology, Fuchu, Japan, in 2011. In 2011, he joined Railway Technical Research Institute, Tokyo, Japan. His research interests are in the areas of railway wireless system, condition monitoring system and graph theory. He is a member of the Institute of Electrical Engineers of Japan and Information Processing Society of Japan.

Nariya Iwaki received the B.Eng. degree in civil engineering from the Daido Institute of Technology, Nagoya, Japan, in 2008, and the M.Eng. degree in civil Engineering from Gifu University, Gifu, Japan, in 2010. In 2010, he joined JR Central Consultants Company (JRCC), Japan. From 2017 to 2019, he was a Researcher with Railway Technical Research Institute, Tokyo, Japan. He is currently a Senior Staff Engineer with JRCC. His research interests are in the condition monitoring systems for railway facilities.

Kazuki Nakamura (M'00) received the B.Eng. and M.Eng. degrees in electrical engineering from the Musashi Institute of Technology, Tokyo, Japan, in 1998 and 2000, respectively. In 2000, he joined Railway Technical Research Institute, Tokyo, Japan. He is currently a Senior Chief Researcher, Head of Telecommunications and Networking Laboratory. His research interests are communication systems and EMC for railways. He is a Expert Member of the IEC/CISPR/B/WG2, and a member of the Institute of Electronics, Information and Communication Engineers, Institute of Electrical Engineers of Japan, and Institution of Railway Signal Engineers.

Kunihiro Kawasaki (M'09) received the B.Eng. degree from the Faculty of Science and Technology, Keio University, Tokyo, Japan, in 1986. In 1986, he joined Railway Technical Research Institute, Tokyo, Japan. He is currently a Director, Head of Signalling and Transport Information Technology Division. His research interests are communication systems and EMC for railways. He is an Expert Member of the IEC/CISPR/B/WG2, a Liaison Officer of IEC/TC9, and a member of the Institute of Electronics, Information and Communication Engineers and Institute of Electrical Engineers of Japan.

Naoki Kanada received the B.S. degree from the Department of Physics, Tokyo Institute of Technology, Tokyo, Japan, in 1997 and the M.E. degree from the Department of Information and Communication Engineering, University of Electro-Communications, Tokyo, Japan, in 1999. Since 2012, he has been working toward the Ph.D. degree at the Waseda University, Tokyo, Japan. In 2002, he joined Electronic Navigation Research Institute (ENRI), Tokyo, Japan. He was a Visiting Researcher at Center for Air Transportation Systems Research, George Mason University in Virginia, Fairfax, VA, USA, from 2006 to 2007. ENRI is now a part of the National Institute of Maritime, Port, and Aviation Technology. His research interests are aeronautical surveillance and communication systems. He is a member of the Institute of Electronics, Information and Communication Engineers, and the Japan Society for Aeronautical and Space Sciences.

Naruto Yonemoto (M'98) received the B.S., M.S., and Ph.D. degrees from Saga University, Saga, Japan, in 1995, 1997, and 2000, respectively. He joined the Electronic Navigation Research Institute (ENRI), Chofu, Japan, in 2000. He was a Visiting Researcher with the Laboratory of Electronic Antennas, and Telecommunications, France from 2005 to 2006. Since 2010, he has been a Visiting Associate Professor with the Tokyo University of Marine Science and Technology University, Japan. He is currently a Principal Researcher with ENRI/MPAT. His research interests include millimeter-wave radar systems and electromagnetic compatibility. He is a member of the Institute of Electronics, Information and Communication Engineers, and EuMA.

Yosuke Sato received the B.E., M.E., and Ph.D. degrees in electrical and electric engineering from Utsunomiya University, Utsunomiya, Japan in 2000, 2002, and 2005, respectively. He joined Hitachi Kokusai Electric Inc., in 2005. He has been involved in the development and design of high-frequency radio communication equipment. His current research interests are millimeter-wave radio communication system and radar technologies.

Masato Fujii joined Kokusai Electric Inc., in 1996. He has been involved in the development and design of radio communication equipment, including the high frequency power amplifiers. His current research interests are microwave/millimeter-wave radio communication systems.

Katsuya Yanatori joined Hitachi Kokusai Electric Inc., in 1990. He has been involved in the development and design of radio communication equipment, including the antenna systems. His current research interest is microwave/millimeter-wave radio communication systems.

Nobuhiko Shibagaki received the B.S. and M.S. degrees in material engineering from the Nagoya Institute of Technology, Nagoya, Japan, in 1985 and 1987, respectively. In 1987, he joined the Central Research Laboratory, Hitachi, Ltd., Tokyo, Japan, where he was engaged in research and development of surface acoustic wave devices for mobile communications. From 2007 to 2016, he was involved with millimeter-wave CMOS devices and communication systems. In 2016, he moved to Hitachi Kokusai Electric and was recently engaged in millimeter-wave communication and radar system application development and research. He is a member of the Japan delegation of the International Telecommunication Union Radiocommunication Sector (ITU-R) and is acting as the Chairman of the drafting group to discuss the FOD detection system using 90 GHz-band and radio over fiber technologies.

Kenichi Kashima joined Hitachi Kokusai Electric Inc., in 1993. He has been involved in the development of high-frequency technology. His current research interests are millimeter-wave devices and millimeter-wave systems.